Tellus
SERIES A
DYNAMIC
METEOROLOGY
AND OCEANOGRAPHY
PUBLISHED BY THE INTERNATIONAL METEOROLOGICAL INSTITUTE IN STOCKHOLM

Tellus (2010), 62A, 591–604

TELLUS

Sensitivity study of heavy precipitation in Limited Area Model climate simulations: influence of the size of the domain and the use of the spectral nudging technique

By JEANNE COLIN[1]*, MICHEL DÉQUÉ[1], RALUCA RADU[2] and SAMUEL SOMOT[1],
[1]*Météo France CNRM/GMGEC CNRS/GAME, 31057 Toulouse, France;* [2]*National Meteorological Administration LNM, Bucharest, Romania*

(Manuscript received 27 October 2009; in final form 21 May 2010)

ABSTRACT

We assess the impact of two sources of uncertainties in a limited area model (LAM) on the representation of intense precipitation: the size of the domain of integration and the use of the spectral nudging technique (driving of the large-scale within the domain of integration). We work in a perfect-model approach where the LAM is driven by a general circulation model (GCM) run at the same resolution and sharing the same physics and dynamics as the LAM. A set of three 50 km resolution simulations run over Western Europe with the LAM ALADIN-Climate and the GCM ARPEGE-Climate are performed to address this issue. Results are consistent with previous studies regarding the seasonal-mean fields. Furthermore, they show that neither the use of the spectral nudging nor the choice of a small domain are detrimental to the modelling of heavy precipitation in the present experiment.

1. Introduction

Over Europe, intense precipitation episodes are among the most destructive weather events in terms of human losses and material damages. Consequently, the possible evolution of their frequency and/or intensity in the context of climate change is of great concern. A number of studies addressed this issue by presenting climate change scenarios (e.g. Sánchez et al., 2004; Semmler and Jacob, 2004; Gao et al., 2006; Christensen and Christensen, 2007; Beniston et al., 2007; Boberg et al., 2009). Overall, they suggest a future increase of extreme rainfall in northern Europe in summer as well as in winter, whereas in the South, extreme summer precipitation in the Mediterranean region would become more frequent (for complete review on this specific region, see Giorgi and Lionello, 2007). Nonetheless, there are still efforts to be put in the assessment of our abilities to simulate such features in present-day climate. Research has been led to determine their sensitivity to some of the sources of uncertainties implied in their modelling at climatic time scales. For example, Räisänen and Joelsson (2001) compared the modelling of extreme precipitation in two regional climate models, Boberg et al. (2009) further questioned this issue by considering the precipitation spectra in the PRUDENCE ensemble, Schmidli et al. (2007) assessed the respective performances of several statistical and dynamical downscalings of precipitation over the European Alps and Déqué and Somot (2008) focused on the impact of a model's resolution on its representation of extreme precipitation over France. However, these sensitivity studies have not covered all the sources of uncertainties yet. In particular, the respective influences of the domain size and the use of the spectral nudging technique in regional climate models (RCMs) on heavy rainfall have not been thoroughly investigated yet.

Most of heavy precipitation events involve small-scale processes and local orography effects which cannot be taken into account with coarse meshes. For this reason, global circulation models (GCMs) are unable to represent them properly. Indeed, performing global simulations covering long periods of time is still computationally too expensive to allow resolutions finer than 100 km. This limit may not prevent GCMs from successfully reproduce large-scale features of climate but it makes GCMs inadequate tools to simulate local characteristics. Since regional climate modelling issues have drawn an increasing attention over the past two decades, several ways to produce affordable high-resolution simulations over a given area of interest have been designed. Here, we only consider the most popular and commonly used one: limited area models (LAMs). And we

*Corresponding author.
e-mail: jeanne.colin@cnrm.meteo.fr
DOI: 10.1111/j.1600-0870.2010.00467.x

question some of the specificities of this method, regarding the simulation of heavy rains.

The LAM technique consists in nesting a limited-area circulation model inside a coarser GCM. The global synoptic circulation is prescribed by the GCM through lateral boundary conditions (LBC) and the LAM computes the weather evolution within its domain at a higher resolution. LAMs were first developed some 40 yr ago and have been used for climate purposes for 20 yr. Several studies then demonstrated they were able to improve the simulation of local features (e.g. Giorgi and Bates, 1989; Giorgi, 1990; Jones et al., 1995) and they have been further refined and validated with observations ever since (e.g. McGregor, 1997; Giorgi and Mearns, 1999; Bärring and Laprise, 2005). However, since this approach has a relatively short history, there is still much to explore in its limitations and the additional sources of uncertainties and specific difficulties it arouses (de Elía et al., 2008).

In particular, it appeared that nested models could produce large scales significantly different from those imposed by the LBC. Whether this effect should rather be considered as a desirable added value or a detrimental drawbacks is still open to criticism (see Lorenz and Jacob, 2005; Laprise et al., 2008; Alexandru et al., 2009). Indeed, it is not clear whether LAMs might improve the prescribed large-scale or necessarily degrade it in the case they actually affect it. However, in order to limit these potential errors in the use of LAMs, it has been proposed to relax the long waves within the domain towards those of the driving model, in addition to the forcing at the lateral boundaries. This technique, named Spectral Nudging, was initially designed by Waldron et al. (1996) and later developed by von Storch et al. (2000) and Biner et al. (2000). Its strengths and efficiency to reduce LAM large-scale error has been pointed out in several studies (e.g. Miguez-Macho et al., 2004; de Elía et al., 2008; Radu et al., 2008). Nevertheless, it is still argued that it might induce detrimental side effects, mainly on the development of the nested model's small-scale features such as extreme precipitation. In Radu et al. (2008), the spectral nudging applied to the wind components and the temperature caused a slightly enhanced negative bias of the upper quantiles of precipitation which was resolved by nudging the specific humidity. Alexandru et al. (2009) found a noticeable decrease in extreme precipitation when using spectral nudging in their set of experiments. However, they only considered the maximum amount of six-hourly cumulated rainfall over their domain and period of integration, and concluded that more work was necessary to confirm the robustness of their result.

Another particularity of LAMs is their sensitivity to the geometry and the location of the chosen domain of computation. This can be explained by the fact the lateral boundary conditions problem is mathematically ill posed as detailed in Miguez-Macho et al. (2004). According to Jones et al. (1995), or Leduc and Laprise (2009) the domain of integration must be wide enough to allow the LAM to develop its small scales. Seth and Giorgi (1998) also indicated that the area of interest should not be too close to the borders in order to keep away boundaries effects. On the other hand, Miguez-Macho et al. (2004) showed the use of large domains were more likely to lead to synoptic scales diverging from the driving model and that this drawbacks could be avoided with the application of a spectral nudging. They consequently recommended to do so when performing LAMs simulations over areas larger than a few thousands kilometres.

This study further investigates these two issues—use of the spectral nudging technique and size of the domain—as far as the representation of intense precipitation events at a climatic timescale is concerned, which, to our knowledge, has never been done in the literature. We aim at answering the following two questions:

(i) Does the spectral nudging technique deteriorate the modelling of these heavy precipitation events?

(ii) Is it preferable to use a relatively large or small domain to properly simulate this feature?

We use the LAM ALADIN-Climate and we focus on the southwestern region of Europe and more specifically on the areas bordering the Mediterranean sea where the most severe events occur. We proceed in a framework similar to the so-called Big-Brother Experiment based on the perfect-model approach developed by Denis et al. (2002) (see also e.g. de Elía et al., 2002; Laprise et al., 2008; Radu et al., 2008; Leduc and Laprise, 2009). It consists in creating an experiment which can be considered as an ideal reference (the Big-Brother run) to which the LAM's simulations are compared. The goal is to isolate the uncertainties due to the nesting method from all other sources of error.

The paper is organized as follows. In Section 2, we describe our methodology: the Big-Brother experimental setup, the models we used, the observed data, and the way we computed the interpolations that were required to compare our simulations. Section 3 shows a brief validation of our Big-Brother simulation. In Section 4, we consider the seasonal mean differences between our pairs of regional simulation and Section 5 details our results concerning intense precipitation. Section 6 is an additional paragraph in which we confirm our conclusions in a less theoretical framework, which correspond to the common use case of LAM. We conclude in Section 7 where we recall our main results and suggest further perspectives.

2. Model, experimental setup and data

In this study, we carry out a set of simulations over Western Europe with the LAM ALADIN-Climate (Radu et al., 2008) at a 50 km resolution. The model is forced with the ERA40 monthly sea surface temperature (SST) (Fiorino, 2004 and lateral boundary conditions provided by the GCM ARPEGE-Climate (Déqué and Piedelievre, 1995; Déqué, 2007).

2.1. *The models*

ALADIN-Climate can actually be considered as a version of ARPEGE-Climate since they share the same computer code. Therefore, they can be run with the same physical parametrizations and dynamical schemes. ARPEGE-ALADIN-Climate is a spectral, semi-implicit and semi-Lagrangian model. In this study, we use its last version (V5.1), which has been recently released. The major characteristics of the physics and dynamics mentioned in Radu et al. (2008) remain valid for the present version and more details about ALADIN-ARPEGE-Climate V5.1 can be found at http://www.cnrm.meteo.fr/gmgec/arpege-climat/ARPCLI-V5.1/index.html.

2.2. *The idealised framework*

As explained in Section 1, we chose a perfect-model type of approach. Our method is almost equivalent to the one detailed in Radu et al. (2008) except that we use the next version of the model and that our Big-Brother simulation is run with a different configuration of ARPEGE-Climate. Here is how we proceeded.

First, we performed a 23-yr-long global simulation (ARP50) in present-day climate (1979–2001) with a variable resolution version of ARPEGE-Climate. The geometric configuration we used is similar to the one described in Gibelin and Déqué (2003). We just recall here some relevant features: the spectral truncation is T159, with 31 vertical levels located mainly in the troposphere. The pole of stretching is located at the centre of the Mediterranean basin (40°N, 12°E) and the stretching factor is 2.5. The grid has 160 pseudo-latitudes and 320 pseudo-longitudes. As a result, the maximum horizontal resolution reaches 50 km over Europe and has a minimum of 300 km in the Pacific.

Then we filtered out the small scales of the ARP50's fields to create coarser resolution (around 300 km) LBC we used to force ALADIN-Climate. This driving of ALADIN-Climate through low resolution LBCs consists in imposing the large-scale prognostic variables at the boundaries of the LAM's domain every 6 h. We follow the classical Davies relaxation scheme (Davis, 1976) based on a spatial interpolation of the variables in a buffer zone around the domain (see Fig. 1 for the buffer zone).

ARP50 constitutes the 'virtual reality' we consider as an ideal reference in the comparison of our regional simulations. In other words, our ALADIN-Climate simulations will not be validated against a climatology but compared to ARP50. This approach relies upon the assumption that we cannot expect ALADIN-Climate to reach better performances than ARP50 in its domain of computation. In other words, we presume that a minimum error due to the LAM's configuration and the nesting technique leads to a minimum difference between the regional simulation and the global ARP50 run. Even though ARP50 can not be considered as a truly perfect Big-Brother, we think this hypothesis is reasonable since ALADIN-Climate and ARPEGE-Climate both

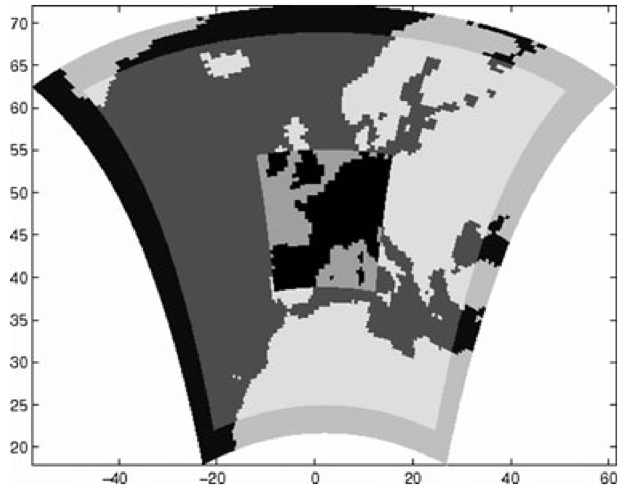

Fig. 1. Domains of integration for the ALADIN-Climate runs. Large domain: EUB50 (buffer zone shown). Small domain: FRB50.

use a resolution of 50 km over the area of interest and share the same physics and dynamics.

2.3. *The set of regional simulations*

Three ALADIN-Climate experiments are run over the 1979–2001 period with the 300 km resolution LBCs.

1. *FR50:* run over a relatively small domain.
2. *EU50:* run over a bigger domain, twice as large as the previous one.
3. *EU50-n:* run over the large EU50 domain, using the spectral nudging technique.

The two domain sizes we chose correspond to commonly used extensions in regional climate modelling over Europe. The size of EU50's domain is equal to the one defined for the intercomparison project FP6-ENSEMBLES, whereas the FR50 one matches those used in projects focusing on the modelling of local climate features at high resolutions, such as the FP6-CECILIA and the ANR-SCAMPEI projects. Both our domains are squared and centred at the same point (47°N, 2°E) so that their meshes overlap. FR50 (respectively EU50) has 37 × 37 grid points—53 × 53 including the buffer zone (respectively 101 × 101 and 117 × 117 grid points) which corresponds to a domain size of approximatively 2000^2 km^2 (respectively 5000^2 km^2) (see Fig. 1). Thus the area of interest of this study is the central zone of the smaller domain. All the following results are presented and analysed over this region only.

All details concerning the spectral nudging of ALADIN-Climate towards ARPEGE-Climate can be found in Radu et al. (2008). In the EU50-n simulation, we nudge all prognostic variables with the following e-folding times: the wind's vorticity (6 h) and its divergence (48 h), the temperature (24 h), the surface pressure (24 h) and the specific humidity (24 h). The function we used is quite simple. There is no relaxation below the 880 hPa pressure level, a linear increase between 880 and 750 hPa, and a constant rate above. Similarly, the wavelengths shorter than 300 km remain free, the full nudging is applied to the ones longer than 400 km with a linear transition in between. Compared to other studies, this spectral nudging can be considered as rather constraining in terms of dimensions and variables involved. Generally, only scales larger than approximately 1000 km are nudged, with a bottom limit ranging from 850 to 500 hPa (Alexandru et al., 2009) and it is not a frequent practice to nudge all prognostic variables. This was a deliberate choice, since we intended to investigate the drawbacks of the nudging's constraints.

2.4. *The data*

The ARP50 simulation is validated against the CRU2.1 global time-series (Mitchell and Jones, 2005). The CRU2.1 dataset provides monthly averaged atmospheric variables from 1901 to 2002, gridded at a 0.5° resolution over land areas only. Here, we use the 2-m temperature and precipitation for the 1979–2001 period.

In addition, we use the SAFRAN high-resolution analysis (Quintana Seguí et al., 2008), in order to briefly assess the ARP50's performances in simulating heavy precipitation. The SAFRAN analysis consists of 8 km × 8 km gridded hourly interpolated data over France for the 1958–2008 period. In this study, we consider daily precipitation.

2.5. *The interpolation methods*

The ARPEGE-Climate grid used for ARP50 differ from those of the CRU2.1 and SAFRAN datasets, and does not superimpose to the ALADIN-Climate ones either. As a consequence, the validation of ARP50 and the comparison of FR50, EU50 and EU50-n to ARP50 both require to perform interpolations of the models outputs.

For the validation part (Section 3), we carry out a barycentric interpolation of the ARP50 fields over the CRU2.1 and SAFRAN grids: for each grid point of the climatology, we compute a weighted mean of the nearest three points of the ARPEGE-Climate's grid. And we do so for each diagnosis we consider, that is to say the seasonal-mean precipitation and temperature, and the upper quantiles of daily precipitation. The same method is used for the comparison of our regional simulations (FR50, EU50 and EU50-n) to the Big-Brother (ARP50) (Sections 4 and 5) where we interpolate the results of ARP50 over the FR50's grid, which happens to be a subgrid of the EU50 and EU50-n one.

This kind of calculation usually raises no problem when comparing mean fields. But it can be detrimental to the evaluation of extreme events, especially when the resolutions are different—as it is the case with ARP50 and SAFRAN—since it may result in a smoothing effect of the interpolated fields. In order to remain as objective as possible in our validation of ARP50 regarding this matter, we perform a second type of interpolation we will refer to as the 'nearest neighbour' one: for each grid point of ARP50 located in the SAFRAN domain, we compute the difference between the upper quantiles of ARP50 and those of the nearest SAFRAN grid point. The comparison of FR50, EU50 and EU50-n to ARP50 is less problematic since the resolutions of ALADIN-Climate and ARPEGE-Climate we used are equals even though the meshes do not overlap. Nonetheless, we also carry out another comparative analysis where no spatial interpolation is performed (see Section 5.2).

3. Validation of the ARP50 simulation against reality

Although the so-called perfect-model approach implies to compare results to the 'virtual reality' (Big-Brother) instead of the observed reality, it would make little sense if the Big-Brother's simulated climate were too different from the observed one. Consequently, we first need to make sure the ARP50 simulation is realistic enough to enable the use of an idealised framework. We do so by comparing ARP50 to the CRU2.1 climatology above-mentioned. Such a validation involves the choice of a benchmark setting the level of differences to the climatology which are acceptable regarding this matter. The state of the art in regional climate modelling at a resolution 50 km over Europe provides a relevant reference.

3.1. *Seasonal means*

Table 1 indicates the spatially mean biases and spatial root mean square errors (RMSE) of ARP50 against CRU2.1 over the area of interest (FR50) for the four following seasons: winter (DJF), spring (MAM), summer (JJA) and autumn (SON). The temperature mean bias is negative and inferior to 1 °C except in spring where it reaches −1.5 °C. The RMSE stay under 2 °C. The daily precipitation biases range from −0.3 mm d^{-1} (SON) to

Table 1. Comparison of ARP50's seasonally averaged 2-m temperature (°C) and Precipitation (mm d^{-1}) against CRU2.1 data (ARP50 - CRU2.1), over the FR50 domain: spatially averaged biases and root mean squared errors

	2-m temperature (°C)		Precipitation (mm d^{-1})	
Season	Bias	RMSE	Bias	RMSE
Winter (DJF)	−0.5	1.5	0.6	1.3
Spring (MAM)	−1.5	1.9	0.6	1.1
Summer (JJA)	−0.5	1.1	0.2	0.8
Autumn (SON)	−0.8	1.5	−0.3	1

Table 2. Comparison of ARP50's heavy precipitation against SAFRAN database (ARP50 - SAFRAN), over the SAFRAN domain (France), using the barycentric interpolation: mean observed values, spatially averaged biases and root mean squared errors of the 95% and 99% quantiles of Daily Precipitation (mm d^{-1})

	95% Quantile (mm d^{-1})			99% Quantile (mm d^{-1})		
Season	SAFRAN	Bias	RMSE	SAFRAN	Bias	RMSE
Winter (DJF)	13.6	0.7	4.6	24.6	−1	8.2
Spring (MAM)	12.2	−0.3	3.3	22.4	−0.9	5.2
Summer (JJA)	11.5	−3.2	4	23.6	−4.2	6.7
Autumn (SON)	15	−3	5.3	30	−5.4	10.2

0.6 mm d^{-1} (winter and spring), the RMSE is close to 1 mm d^{-1} for all seasons. These results are similar to those found in the regional climate modelling literature (e.g. Gibelin and Déqué, 2003; Giorgi et al., 2004; Somot et al., 2008; see also chapter 11 of the 4th Assessment IPCC Report, 2007 at http://www.ipcc.ch/publications_and_data/ar4/wg1/en/ch11.html). In particular, the biases are not larger than those computed for 10 RCMs in the PRUDENCE project (Jacob et al., 2007).

3.2. *Extremes of precipitation*

Since this paper focuses on the extreme precipitation feature, we now examine ARP50's performances in simulating it. We compute the differences of upper quantiles of precipitation between ARP50 and SAFRAN following the two interpolation methods explained in Section 2.5. Table 2 proceeds from the barycentric interpolation of ARP50's quantiles over the SAFRAN's grid. For each season, it gives the SAFRAN's 95 and 99% daily precipitation quantiles and the corresponding spatial bias and RMSE between ARP50 and SAFRAN. Table 3 displays the equivalent results obtained with the nearest neighbour interpolation method over the ARP50's grid.

It appears that both methods give similar results: ARP50 notably underestimates the heaviest precipitation events, in particular during the summer and autumn seasons. To take a closer look at these differences, we considered their spatial repartitions by plotting maps of relative differences of the same quantiles (not shown). It revealed that the larger errors were located over mountains and in Southeast France, around the Mediterranean sea where the most severe events take place. Elsewhere, they stay inferior to −20%. This pattern is in good agreement with the state of the art (see Semmler and Jacob, 2004; Ricard et al., 2009). The rather poor results of ARP50—as any RCM at this resolution—over the aforementioned regions can be explained by their complex orography insufficiently represented at a 50 km resolution and the importance of very small-scale non-hydrostatic processes (Ducrocq et al., 2008) which are not resolved in any climate model. However, this does not mean RCMs are by no means unable to capture any features of this kind of events. The French project CYclogénèse et PRécipitations Intense en Région Méditerranéenne (CYPRIM) showed that it is possible to successfully reproduce the occurrence of these catastrophic rainfall events (above 200 mm d^{-1}) with the high-resolution non-hydostatic model MESO-NH forced by ARPEGE-Climate with an appropriate selection of synoptic-scale situations in the climate run. This means that ARPEGE-Climate is able to properly simulate the triggering features of the mesoscale processes involved in these events of extreme rainfall (Beaulant, personal communication). Furthermore, it happens that the appropriate situations selected in CYPRIM with statistical methods (considering pressure and moisture-flow parameters) match the ARPEGE-Climate extremes of precipitation (Somot, personal

Table 3. Comparison of ARP50's heavy precipitation against SAFRAN database (ARP50 - SAFRAN), over the SAFRAN domain (France), using the 'nearest neighbour' interpolation over the ARP50's grid: mean observed values, spatially averaged biases and root mean squared errors of the 95 and 99% quantiles of Daily Precipitation (mm d^{-1})

	95% Quantile (mm d^{-1})			99% Quantile (mm d^{-1})		
Season	SAFRAN	Bias	RMSE	SAFRAN	Bias	RMSE
Winter (DJF)	13.9	0.6	4.9	25.1	−1.3	8.3
Spring (MAM)	12.6	−0.2	4	23.2	−0.9	6
Summer (JJA)	12.1	−3.3	4.5	24.5	−4.3	7.5
Autumn (SON)	15.3	−2.9	5.7	30.2	−5.4	10.6

communication, 2008) even though the amount of rain are underestimated.

From this short validation section, we conclude that ARP50 constitutes a suitable Big-Brother simulation. Thus, we now consider it as the reference for the rest of the study: in agreement with the idealised framework, the respective performances of the three ALADIN-Climate experiments will be evaluated by comparing each of them to ARP50 only.

4. Comparison of the regional simulations: seasonal-mean temperature and precipitation

A first comparison of the three regional simulations is made by considering their seasonal means of temperature and precipitation, averaged over the 23 yr of integration.

Table 4 presents the spatially averaged biases and RMSE of these seasonal-mean fields with respect to ARP50 (the spatial averages are computed over the land grid points of the common domain, as in Table 1). Except for the EU50's summer temperature, all three ALADIN-Climate experiments are quite similar and show small differences to ARP50. The biases of temperature (respectively precipitation) do not exceed $+1\,^{\circ}$C (respectively -0.3 mm d^{-1}) and the RMSE stay under $+0.8\,^{\circ}$C (respectively $+0.6$ mm d^{-1}).

Figures 2 and 3 show the spatial distribution of winter (DJF) and summer (JJA) differences of the mean 2-m temperature and daily precipitation. For the mean precipitation, FR50 (small domain), unlike EU50 and EU50-n (large domain), shows a significant dry bias in winter (up to -2 mm d^{-1}) close to the western border of its domain, due to a boundary effect. This pattern is also present during summer but it is much weaker, the westerly flow coming from the Atlantic Ocean being enhanced in winter. Apart from this feature, all three ALADIN-climate experiments show similar behaviours and small differences to ARP50 (between -0.5 and $+0.5$ mm d^{-1}) in both seasons.

Concerning the 2-m temperature, FR50 and EU50-n both stay fairly close to the reference in summer as well as in winter. Their respective biases are limited to $\pm 0.5\,^{\circ}$C in winter and reach $+1\,^{\circ}$C ($+1.5\,^{\circ}$C over small areas) in summer. In some very localized spots (in the Alps or along the Mediterranean coast of France) however, all three simulations show a severe negative bias to ARP50 but this is a spurious effect to the differences in the orography of ALADIN-Climate and ARPEGE-Climate grids. Outside these spots, EU50 shows a significant warm bias, especially in summer where it is superior to $+0.5\,^{\circ}$C everywhere except in the Iberian Peninsula and the British Isles and reaches $+2$ to $+4\,^{\circ}$C in some other parts of the area of interest. This pattern is not due to an increased internal variability of the LAM (random error) in the larger domain during summer. There is strong evidence that it rather results from a systematic error. Indeed, it appears in other experiments we have carried out over similar domains (see e.g. Radu et al., 2008), and multiple simulations run with ALADIN-Climate over the ENSEMBLES domain (same size as EU50) show that a random error would at most reach $+1.6\,^{\circ}$C (Sanchez-Gomez, personal communication, 2010). And besides, this warm bias is a well-known feature of other RCMs in Europe (Jacob et al., 2007). The fact that it arises here within the perfect-model paradigm is not easy to interpret. However, this indicates that the bias can not be looked at as an intrinsic defect of the model only (for instance in the treatment of the dynamics, the physical parametrizations or the surface scheme) but is somewhat related to the way the LAM is forced at its boundaries: the LAM produces a solution different from the Big-Brother's. Consequently, the less the LAM is constrained by its forcing, the more its solution is likely to differ. This statement is consistent with the finding of a stronger bias during summer, when the large-scale advection is weaker. And it also explains why the drift is significantly lower over a smaller domain of integration (FR50), or when applying a spectral nudging (EU50-n) as it has already been shown in Radu et al. (2008). Additional investigations would be required to fully explore and understand the reasons why, under certain circumstances, a difference of solution between our LAM and the Big-Brother tends to result in this systematic error, but it would go beyond the scope of this paper. Here, we just confirm former results regarding one of the problems that might occur when running a LAM over a large domain and the ways it can be avoided. We are now going to deal with the possible negative side-effects of the spectral nudging

Table 4. Comparison of FR50, EU50 and EU50-n seasonally averaged 2-m temperature (°C) and Precipitation (mm d^{-1}) against ARP50, over the FR50 domain: spatially averaged biases and root mean squared errors (ARP50 - ALADIN-Climate)

	2-m temperature (°C)						Precipitation (mm d^{-1})					
	Bias			RMSE			Bias			RMSE		
Season	FR50	EU50	EU50-n	FR50	EU50	EU50-n	FR50	EU50	EU50-n	FR50	EU50	EU50-n
Winter (DJF)	−0.03	0.2	−0.1	0.7	0.8	0.7	−0.08	−0.001	0.04	0.6	0.6	0.6
Spring (MAM)	0.05	0.3	0.03	0.6	0.7	0.6	−0.1	−0.1	0.03	0.6	0.6	0.6
Summer (JJA)	0.4	1	0.4	0.8	1.3	0.8	−0.1	−0.3	−0.2	0.5	0.6	0.5
Autumn (SON)	0.05	0.3	−0.02	0.7	0.8	0.6	−0.13	−0.2	−0.05	0.6	0.6	0.5

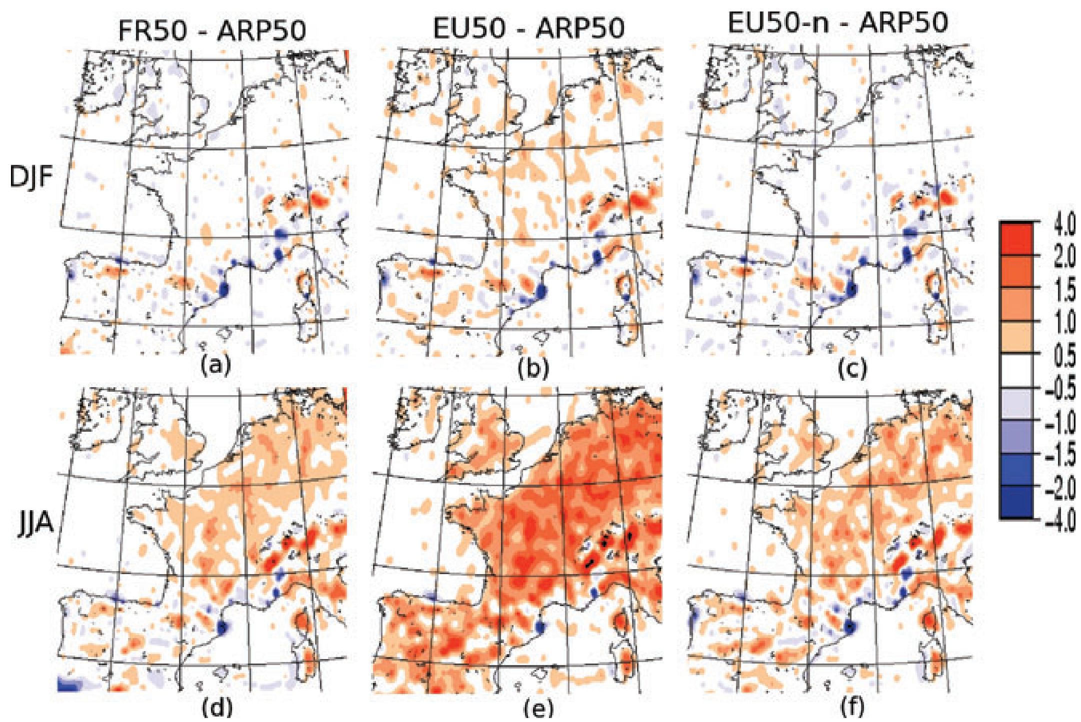

Fig. 2. Mean winter (DJF) 2-m temperature (°C) differences to ARP50 for: (a) FR50, (b) EU50, and (c) EU50-n. (d), (e), (f) are the respective fields for the summer (JJA) season.

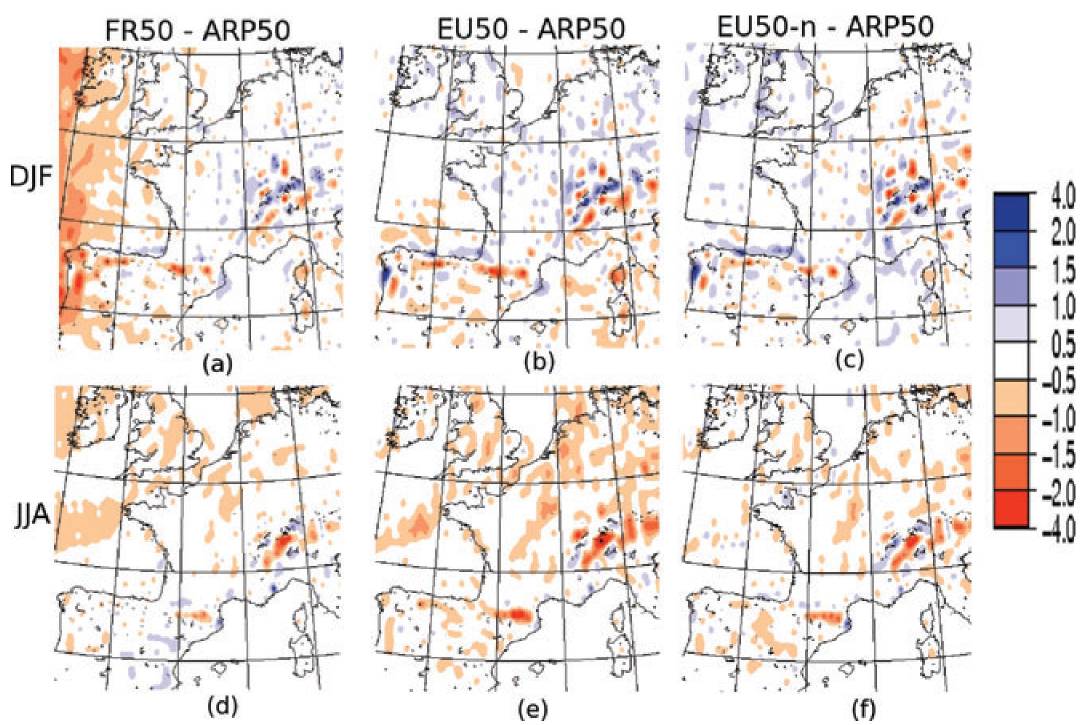

Fig. 3. Same as Fig. 2 for daily precipitation (mm d^{-1}).

and/or the use of a smaller domain could have on the modelling of extreme precipitation.

5. Comparison of the regional simulations: intense precipitation events

5.1. Spatial patterns

As we did in Section 3.2 with ARP50 and the SAFRAN database, we compute the 95–99% quantiles' differences between the ALADIN-Climate simulations and ARP50. Here, we only show the results obtained with the barycentric interpolation over the ALADIN-Climate grid.

Table 5 presents the seasonal-mean biases and RMSE of these differences, spatially averaged over the common domain. Overall, FR50, EU50 and EU50-n stay fairly close to ARP50 for this feature. FR50 and EU50 slightly underestimate both quantiles (with biases staying under the local maxima of −10% for the 95% quantile, and −16% for the 99% quantile) whereas EU50-n overestimates the 95% quantile except in summer and underestimate the 99% quantile except in winter (with similar absolute values of biases).

We also consider the spatial patterns of intense precipitation. Figure 4 shows the relative differences (in percentage) to ARP50 of daily precipitation's 99% quantiles (mm d^{-1}) for two extended seasons: winter and spring (DJFMAM) we will refer to as the advective season, and summer and fall (JJASON) we will refer to as the convective season. We added the 99% quantile field of ARP50 on its original grid for both seasons (Figs. 4a and b).

We define these seasons because over the region of interest, most the heavy rainfall occurring in winter and spring are due to synoptic-scale disturbances whereas in summer and autumn they are mainly caused by convective storms. Furthermore, this choice of seasons follows the pattern of ARP50 high and low bias from SAFRAN heavy precipitation, as shown in Section 3.2.

In the advective season, noticeable differences to ARP50 can be found in the western part of the common domain (Portugal, Western Spain and Ireland), in Western France, Corsica and Sardinia. At the western border, FR50 rather strongly underestimates intense precipitation (up to −40%) as it does for the whole spectrum because of boundaries effects (see previous section). In Western France, EU50 simulates slightly enhanced heavy precipitation. In Corsica and Sardinia, all three ALADIN-Climate simulations underestimate extreme precipitation and EU50-n shows the smallest bias. Elsewhere, FR50, EU50 and EU50-n's behaviours are similar, close to the one of ARP50.

During the convective season, FR50 shows a negative bias over the western border of the domain which is slightly stronger than in the advective season, in agreement with Figs. 3a and d. On the contrary, FR50 overestimates the 99% quantile over Catalonia whereas EU50 and EU50-n's patterns are not clear-cut. EU50 no longer simulates enhanced precipitation over Western France but it significantly lessens intense precipitation in the northeastern corner of the common domain. Differences on Corsica and Sardinia have the same sign as in the advective season but seem to be slightly larger.

Many other indexes can be computed. Basically, one can either consider precipitation over a given threshold (numbers of days for which the precipitation is above the threshold, mean precipitation superior to the threshold, etc.) or calculate upper quantiles of precipitation. Thoroughly examining all these indicators, we found no more additional significant information.

From this first analysis, it appears that except by the western and eastern boundaries of our common domain, the differences are quite small. Yet, the signal is rather unclear around the Mediterranean sea. In order to further investigate the strengths and weaknesses of our experiments over this region in terms of heavy precipitation, we now consider another approach based on quantile–quantile diagrams.

5.2. Quantile–quantile analysis

Quantile–quantile diagrams can either be plotted on grid points or over boxes. The second approach has two advantages: it allows a more systematic comparison than single random points and offers a possibility to avoid any interpolating potential side effects with the use of the so-called 'pooling' method

Table 5. Comparison of FR50, EU50 and EU50-n's heavy precipitation against APR50, over the FR50 domain: mean observed values, spatially averaged biases and root mean squared errors of the 95 and 99% quantiles of Daily Precipitation (mm/day) (ARP50 - ALADIN-Climate)

	95% Quantile (mm d^{-1})							99% Quantile (mm d^{-1})						
		Bias			RMSE				Bias			RMSE		
Season	ARP50	FR50	EU50	EU50-n	FR50	EU50	EU50-n	ARP50	FR50	EU50	EU50-n	FR50	EU50	EU50-n
Winter (DJF)	13	−0.6	−0.2	0.2	2	1.6	1.6	21.9	−0.6	−0.05	0.2	2.9	2.7	2.4
Spring (MAM)	10.2	−0.5	−0.3	0.03	1.5	1.5	1.5	19	−1	−0.4	−0.2	2.6	2.6	2.2
Summer (JJA)	7.3	−0.6	−0.8	−0.3	1.2	1.5	1.2	16	−1.2	−1.6	−0.9	2.7	3	2.4
Autumn (SON)	11.8	−0.7	−0.6	0.3	1.8	1.7	1.5	23.3	−1.2	−0.6	−0.3	3.8	3	2.8

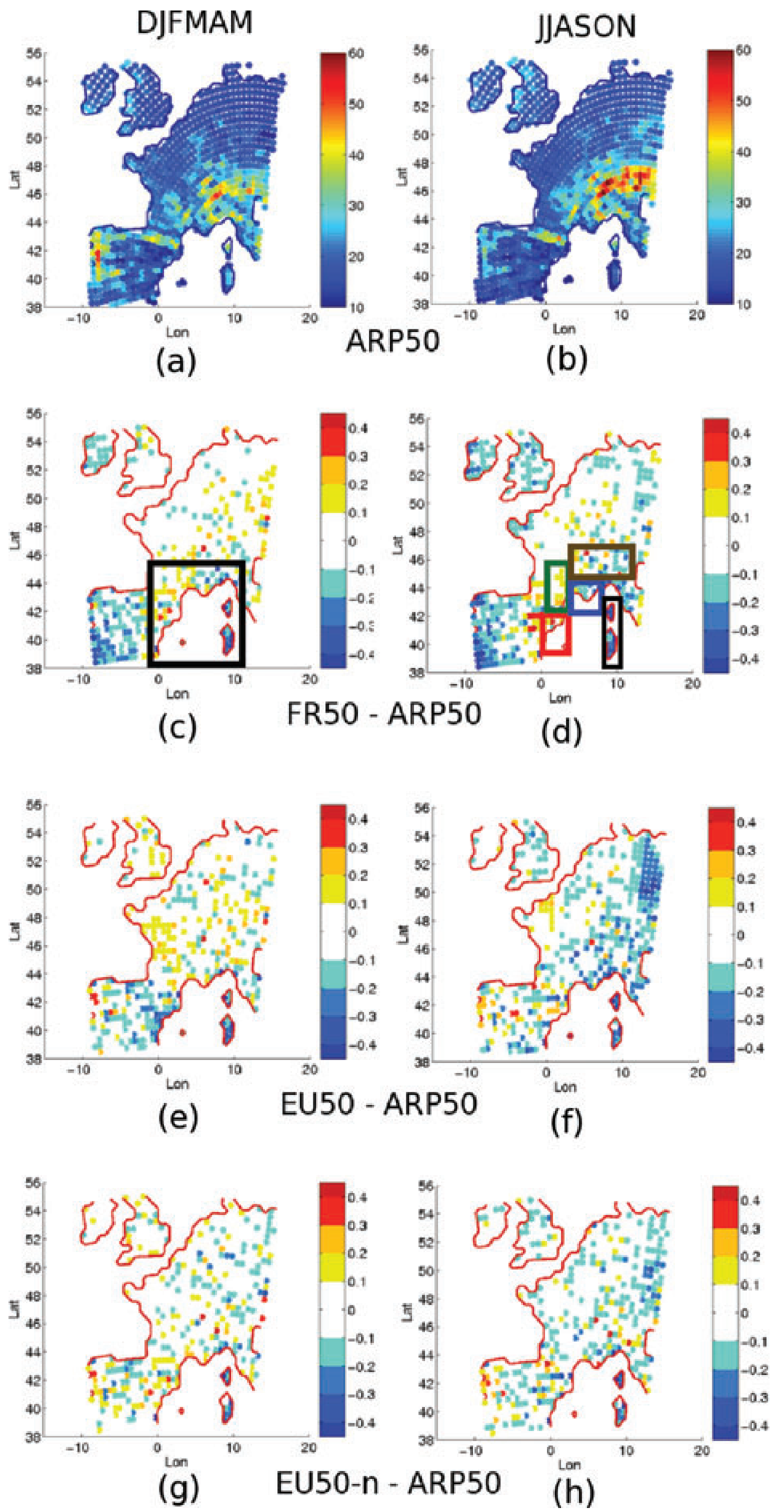

Fig. 4. Advective (DJFMAM) (left-hand panel) and convective (JJASON) (right-hand panel) 99.9% quantiles of daily precipitation (mm d^{-1}). (a) and (b) show the ARP50 99.9% quantile for each season. Advective season's relative differences to ARP50 are plotted for: (c) FR50, (e) EU50, and (g) EU50-n. (d), (f), and (h) are the same fields for the convective season. (c) and (d) also show the boxes for the quantile–quantile diagrams in Figs. 5 and 6. The large box *Medit* is drawn on (c). (d) displays the smaller boxes, drawn on the same plot: *Catalonia* in red, *Roussillon* in green, *Provence* in blue and *Alps* in black.

(Déqué and Somot, 2008). Within a given box, we sort the daily precipitation of all grid points for each simulation (ALADIN-Climate and ARPEGE-Climate) on its original grid, regardless of the days of occurrence. Then we select quantiles from this sorted series to obtain quantile–quantile diagrams of FR50, EU50 and EU50-n versus ARP50. According to Déqué and Somot (2008), this method is more adequate to compare extreme parameters of simulations run at different resolutions. But although this is not

Table 6. Characteristics of the quantile–quantiles boxes: coordinates of the boundaries and number of grid points

Boxes	West longitude	East longitude	South latitude	North latitude	ARPEGE-Climate number of grid points	ALADIN-Climate number of grid points
Medit	0	10E	38N	46N	146	126
Catalonia	1W	4E	40N	42N	23	18
Roussillon	2E	4E	42N	46N	24	27
Provence	4E	8E	42N	45N	27	19
Alps	6E	12E	45N	48N	74	60
Corsica-Sardinia	0E	10E	38N	43N	15	13

the case in this study, we do have different grids and this method also constitutes a satisfying solution in our case.

In order to take a closer look at the some of the regions surrounding the Mediterranean sea in our domain, we define 6 boxes: a rather large box we call *Medit* (shown in Fig. 4c) and several smaller ones (shown in Fig. 4d), as spatially homogenous as possible regarding the intense precipitation parameter. Table 6 details the exact coordinates of their boundaries and the number of grid points they include.

Figure 5 presents the convective (JJASON) quantile–quantile diagrams (ALADIN-Climate runs versus ARP50, quantiles per thousand) over each box, and Fig. 6, the same plots for the advective season (DJFMAM). Overall, FR50, EU50 and EU50-n all stay fairly close to the ARP50 reference over the whole spectrum of precipitation, except in Corsica and Sardinia. Over the large box *Medit* (a), all simulations slightly underestimate heavy rains with enhanced differences in the convective season. EU50-n shows the smallest errors and EU50 the largest, FR50 being in between. We find similar behaviours over *Provence* (d) and *Alps* (e). In *Catalonia* (b) and *Roussillon* (c), the results are a little different: In the advective season, EU50-n overestimates precipitation heavier than approximately 7 mm d^{-1} which corresponds to the 95% quantile whereas EU50 largely underestimates rainfall superior to 5 mm d^{-1} (90% quantile) and FR50 stays close to ARP50. During the convective season on the contrary, FR50 overestimates the upper quantiles (over 98%) whereas EU50 and EU50-n both simulate fairly good extremes, except for the very last quantiles. Finally, the *Corsica-Sardinia* box (f) shows a specific pattern: During the advective season, FR50, EU50 and EU50-n stay quite close, with negative differences to ARP50 larger than in any other box, from the 95% quantile to the tail of the spectrum. This result is probably induced by the fact that the representation of the complex orography and land–sea mask of these two small islands are quite different in ALADIN-Climate and ARPEGE-Climate. In the convective season however, EU50 and EU50-n both underestimate intense precipitation over the 99% quantile in the same extent they do over *Provence* (d) (that is to say, less than -5 mm d^{-1}), but FR50's bias is much stronger and exceeds -10 mm d^{-1} for the last quantiles. We know that during this season, many of the high precipitation events occurring over *Corsica-Sardinia* (as well as over *Catalonia*, *Provence* and *Roussillon*) are associated with a easterly, or southeasterly, synoptic flow (Nuissier et al., 2008). The relatively poor performances of FR50 in simulating heavy rainfall over this area and for this season, compared to EU50 and EU50-n, can therefore be explained by the eastern border's vicinity in this region for the small domain. And the fact that this defect of FR50 does not appear in the other boxes, located further west, suggests the eastern boundary effect's extension is limited to this region.

To summarize, we can say that except over small areas such as Catalonia, and over Corsica and Sardinia, our three ALADIN-Climate simulations show very similar patterns of heavy precipitation. And this applies to both seasons, although all simulations underestimate extremes more in the convective season than in the advective one.

From these results, we can conclude that in this study, the use of the spectral technique nudging technique does not degrade the modelling of extreme precipitation. It even seems to improve it over some areas, as shown in the previous section, but the differences are rather small and more work would be required to test their significance. Anyway, whether this improvement is meaningful or not, our results constitute a rather positive support of the spectral nudging since we found it allowed to reduce mean biases without deteriorating the simulation of extreme precipitation.

Regarding the size of the domain, it turns out the small area of integration is not detrimental either to the representation of intense precipitation, except in the vicinity of the western boundary through which the large-scale flow mainly enters the domain, and very close to the eastern border from which come some of the synoptic-scale systems affecting heavy precipitation in South-eastern France and Sardinia. On the contrary, heavy precipitation tends to be underestimated in some regions of the large domain which could be explained by the errors found on seasonal-mean biases.

6. Low resolution forcing

We believe the perfect-model method we adopted for this study was necessary to come to safe conclusions. However, in order

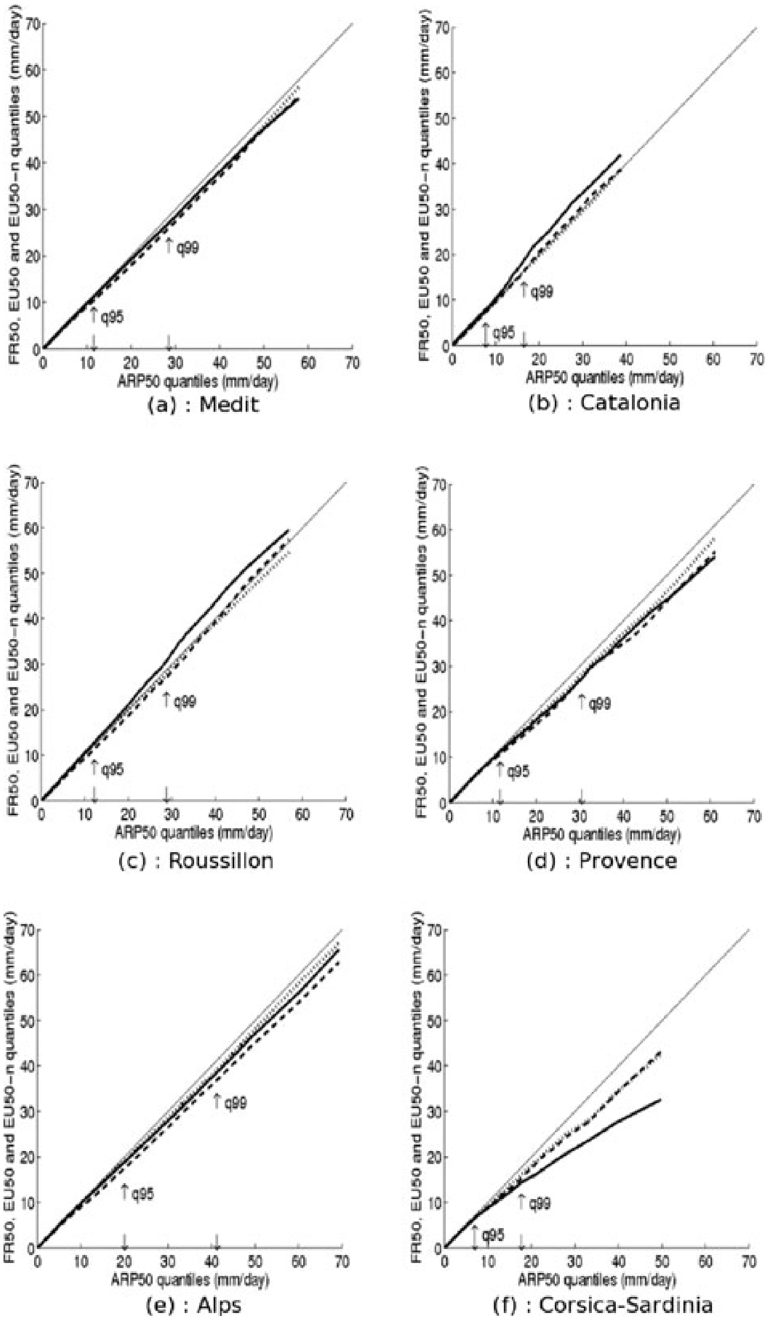

Fig. 5. Convective (JJASON) quantile–quantile (per thousand) plots (mm d^{-1}) over the boxes shown in Figs. 4c and d: (a) Medit, (b) Catalonia, (c) Roussillon, (d) Provence, (e) Alps, (f) Corsica-Sardinia. ARP50 quantiles are sorted along *x*-axis and ALADIN-Climate's one along the *y*-axis. FR50: solid line; EU50: dashed line; EU50-n: dotted line.

to validate our results in a more realistic case, we have also forced ALADIN-Climate with a real T63 (300 km resolution) ARPEGE-Climate global experiment, and compared the results with our ARP50 Big-Brother.

Indeed, LAMs are intended to downscale low-resolution simulations that contain no small-scale information whatsoever. Yet, in this framework, even though ARP50 emulates a coarse resolution, its large scales developed with the fine-resolution information. Our results may thus be biased by the fact that it might be easier for ALADIN-Climate to simulate valid small-scale features when its low-resolution forcing is perfectly consistent with those. And a similar objection may be raised concerning the domain's size. This possible weakness of our study refers to the question of whether the small scales influence the synoptic circulation or not (see tenet 5 in Laprise et al., 2008). It is not the goal of our paper to address this controversial issue. However, we are willing to verify our conclusions in the case of a regular coarse resolution forcing.

We do not show here the results but simply jump to the conclusion. Although in this case, each ALADIN-Climate experiment

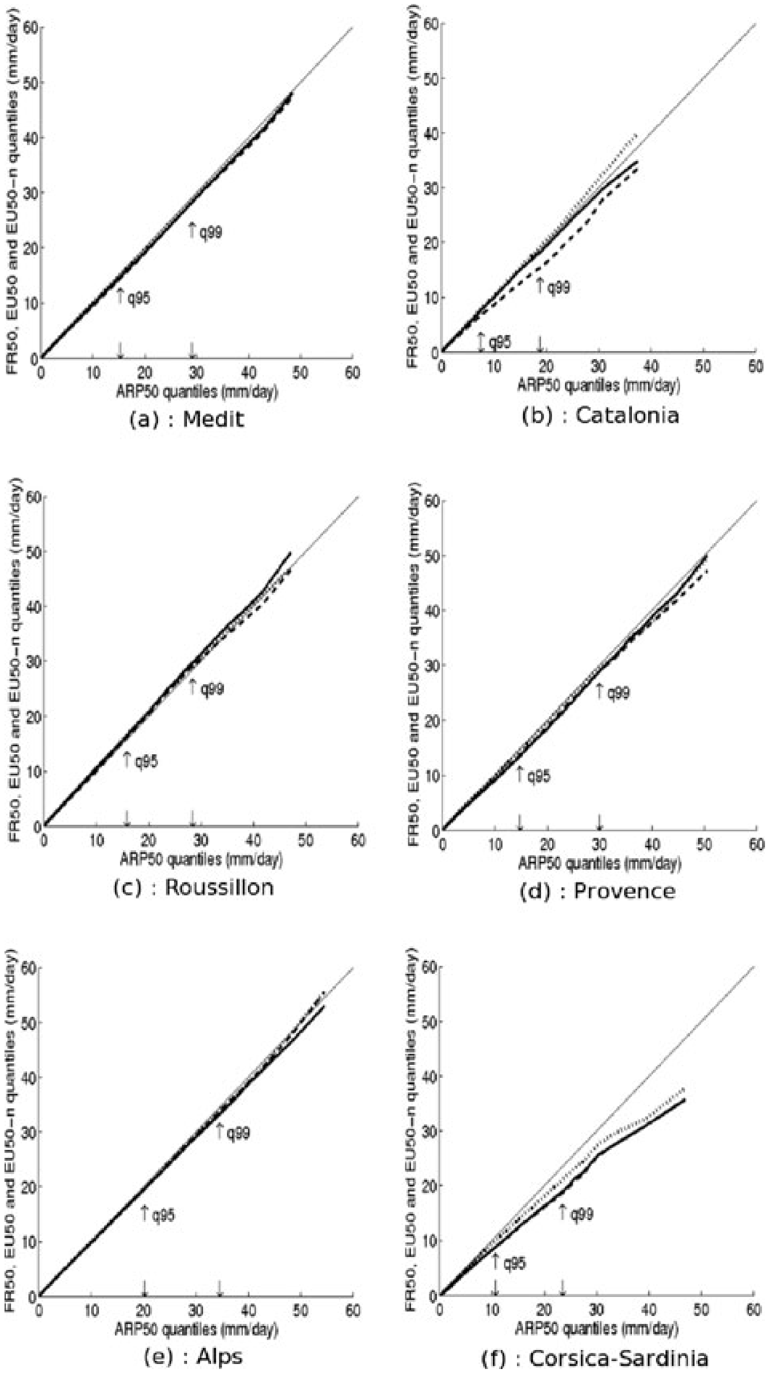

Fig. 6. Same as Fig. 5 for the advective season (DJFMAM).

may show stronger biases to ARP50 regarding extreme precipitation, the results remain the same regarding the sensitivity of the heavy rainfall to the domain size and the use of the spectral nudging technique: a small domain does not prevent the development of intense precipitation in our region of interest, except in the close vicinity of its eastern border, and neither does the spectral nudging.

7. Conclusion

The aim of our study was to assess the impact of two sources of uncertainties in the modelling of extreme precipitation at climatic time scales with the LAM ALADIN-Climate: the size of the domain of integration, and the use of a spectral nudging technique. This objective relates to the following questions:

Is a rather small domain detrimental to the representation of extremes? And does the application of a spectral nudging necessarily degrade the model's ability to generate such events? We addressed both questions with regard to the extremes of precipitation occurring in Western Europe and more specifically around France.

We proceeded with a perfect-model approach close to the Big-Brother Experiment because this method allows to carefully isolate the influence of the designated factors from any other source of uncertainty. As a first step, we performed a global simulation with ARPEGE-Climate at a resolution of 50 km over Europe (the Big-Brother). Then we filtered out its small scales to obtain a low-resolution forcing (300 km) for ALADIN-Climate. Finally, three regional simulations were carried out at a 50 km resolution: one over a small domain of integration (2000^2 km^2) centred over France (FR50), a second one over a larger domain (5000^2 km^2) including the previous one (EU50) and a third one run over the large domain to which we applied a rather strong spectral nudging on all prognosis variables (EU50-n). After having verified our ARPEGE-Climate high-resolution (50 km over Europe) simulation was a suitable Big-Brother run, we analysed the performances of the three ALADIN-Climate runs by comparing each of them to the Big-Brother reference.

Regarding the seasonal-mean fields, the results confirm the conclusions of previous studies conducted on this subject. Indeed, EU50 shows a rather important bias of seasonal 2-m temperature in summer which is significantly reduced in both FR50 and EU50-n, where the differences to the Big-Brother are thus quite similar. This finding indicates that the spectral nudging technique allows to avoid such limitations in the use of rather large domains of integration. Besides, FR50 was found to be too dry in winter over the western border of our area of interest, close to the boundary of the small domain. So, as advised in Miguez-Macho et al. (2004), we recommend not to set the boundaries of the domain at the vicinity of the considered region.

Concerning the extremes of precipitation, all three ALADIN-Climate simulations are quite similar. The most distinct patterns of differences can be linked with the large-scale errors we just detailed: FR50 underestimates the upper quantiles of precipitation close to its western and eastern boundaries and EU50 shows a similar behaviour over the eastern part of the common domain in summer. Elsewhere, we found no evidence that FR50 or EU50-n would be worse than EU50 to this regard.

From these results, we draw two conclusions. The first one is that the application of the spectral nudging technique does not systematically degrade the representation of a climate model's extremes. Although this study cannot be generalized to any model or any region, it questions one of the warnings sometimes made about the use of this technique. In addition, our results suggest that using a small domain may not prevent the model from simulating extremes of precipitation which are at least as valuable as those computed over a much larger area, with the same resolution. This second conclusion contributes to justify the relevance of very high resolution experiments run over small domains, such as in Déqué and Somot (2008) or for the FP6-CECILIA project where ALADIN-Climate is run at a 12 km resolution over France and several Eastern European countries. A perspective of this study could consist in leading further sensitivity tests regarding the added value of the resolution on the modelling of heavy precipitation, by comparing the FR50 simulation to an equivalent experiment at a 12 km resolution.

8. Acknowledgments

This work was partly supported by SCAMPEI (French Program ANR-08-VULN-009-01) and MEDUP (Forecast and projection in climate scenario of Mediterranean intense events: Uncertainties and Propagation on environment. ANR-07-VULN-001). The authors are indebted to Météo-France and ECMWF for providing and maintaining the ARPEGE-IFS code, and to the ALADIN modellers community.

References

Alexandru, A., de Elía, R., Laprise, R., Separovic, L. and Biner, S. 2009. Sensitivity study of regional climate model simulations to large-scale nudging parameters. *Mon. Wea. Rev.* **137**, 1666–1686.

Bärring, L. and Laprise, R. 2005. High resolution climate modelling: assessment, added values and applications. *WMO/TD No. 987* **30**, 7.3–7.4.

Beniston, M., Stephenson, D. B., Christensen, O. B., Ferro, C. A. T., Frei, C. and co-authors. 2007. Future extreme events in European climate: an exploration of regional climate model projections. *Clim. Change* **81**, 71–95.

Biner, S., Caya, D., Laprise, R. and Spacek, L. 2000. Nesting of RCM by imposing large scales. *Res. Activit. Atmos. Oceanic Modell., WMO/TD, No. 987* **30**, 7.3–7.4.

Boberg, F., Berg, P., Thejll, P., Gutowski, W. J. and Christensen, J. H. 2009. Improved confidence in climate change projections of precipitation evaluating using daily statistics from PRUDENCE ensemble. *Clim. Dyn.* **32**, 1097–1106.

Christensen, J. H. and Christensen, O. B. 2007. A summary of the PRUDENCE model projections of changes in European climate by the end of this century. *Clim. Change* **81**, 7–30.

Davis, H. 1976. A lateral boundary formulation for multi-level prediction models. *Quart. J. R. Meteorol. Soc.* **102**, 405–418.

de Elía, R., Laprise, R. and Denis, B. 2002. Forecasting skill limits of nested, limited aera models: a perfect model approach. *Mon. Wea. Rev.* **130**, 2006–2023.

de Elía, R., Laprise, R., Denis, B. and co-authors. 2008. Evaluation of uncertainties in the CRCM-simulated North American climate. *Clim. Dyn.* **30**, 113–132.

Denis, B., Laprise, R., Caya, D. and Cote, J. 2002. Dowscaling abililty of one-way nested regional climate models: the Big-Brother experiment. *Clim. Dyn.* **18**, 107–126.

Déqué, M. 2007. Frequency of precipitation and temperature extremes over france in an anthropogenic scenario : model results and statistical correction according to observed values. *Global Planet. Change* **57**, 16–26.

Déqué, M. and Piedelievre, J. 1995. High-resolution climate simulation over europe. *Clim. Dyn.* **11**, 321–339.

Déqué, M. and Somot, S. 2008. Analysis of heavy precipitation for France using ALADIN RCM simulations. *Idojaras* **112**, 179–190.

Ducrocq, V., Nuissier, O., Ricard, D., Lebeaupin, C. and Thouvenin, T. 2008. A numerical study of three catastrophic precipitation events over southern France. II: mesoscale triggering and stationary factors. *Quart. J. R. Meteorol. Soc.* **134**, 131–145.

Fiorino, M. 2004. A multi-decadal daily sea surface temperature and sea ice concentration data set for the ERA-40 Reanalysis. *ERA-40 Project Report Series* **12**, 1–16.

Gao, X., Pal, J. S. and Giorgi, F. 2006. Projected changes in mean and extreme precipitation over the Mediterranean region from a high resolution double nested RCM simulation. *Geophys. Res. Lett.* **33**, L03706.

Gibelin, A.-L. and Déqué, M. 2003. Anthropogenic climate change over the Mediterranean region simulated by a global variable resolution model. *Clim. Dyn.* **20**, 327–339.

Giorgi, F. 1990. Simulation of regional climate using a limited area model nested in a general circulation model. *J. Climate* **3**, 941–963.

Giorgi, F. and Bates, G. T. 1989. The climatological skill of a regional model over complex terrain. *Mon. Wea. Rev.* **117**, 2325–2347.

Giorgi, F., Bi, X. and Pal, J. 2004. Mean, interannual variability and trends in a regional climate change experiment over Europe. I. Present-day climate (1961-1990). *Clim. Dyn.* **22**, 733–756.

Giorgi, F. and Lionello, P. 2007. Climate change projections for the Mediterranean region. *Global planet. Change* **63**, 90–104.

Giorgi, F. and Mearns, L. O. 1999. Introduction to special section: regional climate modeling revisisted. *Geophys. Res. Lett.* **104**, 6335–6352.

Jacob, D., Bärring, L., Christensen, O. B., Christensen, J. H., de Castro, M. and co-authors. 2007. An inter-comparison of regional climate models in Europe: model performance in present day climate. *Clim. Change* **81**, 31–52.

Jones, R. G., Murphy, J. and Noguer, M. 1995. Simulation of climate change over Europe using a nested regional climate model. I: assessment of control climate, including sensitivity to location of lateral boundaries. *Quart. J. R. Meteorol. Soc.* **121**, 1413–1449.

Laprise, R., de Elía, R., Caya, D., Biner, S., Lucas-Picher, P. and co-authors. 2008. Challenging some tenets of Regional Climate Modelling. *Meteorol. Atmos. Phys.* **100**, 3–22.

Leduc, M. and Laprise, R. 2009. Regional climate model sensitivity to domain size. *Clim. Dyn.* **32**, 833–854.

Lorenz, P. and Jacob, D. 2005. Influence of regional scale information on the global circulation: a two-way nesting climate simulation. *Geophys. Res. Lett.* **32**, L18706.

McGregor, J. L. 1997. Regional climate modelling. *Meteorol. Atmos. Phys.* **63**, 105–117.

Miguez-Macho, G., Stenchikov, G. L. and Robock, A. 2004. Spectral nudging to eliminate the effects of domain position and geometry in regional climate model simulations. *J. Geophys. Res.-Atmos.* **109**(D13104).

Mitchell, T. D. and Jones, P. D. 2005. An improved method of constructing a database of monthly climate observations and associated high-resolution grids. *Int. J. Phys. Climatol.* **25**, 693–712.

Nuissier, O., Ducrocq, V., Ricard, D., Lebeaupin, C. and Anquetin, S. 2008. A numerical study of three catastrophic precipitation events over southern France. I: numerical framework and synoptic ingredients. *Quart. J. R. Meteorol. Soc.* **134**, 111–130.

Radu, R., Déqué, M. and Somot, S. 2008. Spectral nudging in a spectral regional climate model. *Tellus A* **60A**, 2461–2481.

Räisänen, J. and Joelsson, R. 2001. Changes in average and extreme precipitation in two regional climate model experiments. *Tellus A* **53A**, 507–566.

Ricard, D., Beaulant, A.-L., Boé, J., Ducrocq, V., Joly, A. and co-authors. 2009. Impact du changement climatique sur les évènements de pluie intense du bassin Méditerranéen. *La Météorologie* **67**, 19–30.

Sánchez, E., Gallardo, C., Gaertner, M. A., Arribas, A. and Castro, M. 2004. Future climate extreme events in the Mediterranean simulated by a regional climate model: a first approach. *Global Planet. Change* **44**, 163–180.

Schmidli, J., Goodess, C. M., Frei, C., Haylock, M. R., Hundecha, Y. and co-authors. 2007. Statistical and dynamical downscaling of precipitation: an evaluation and comparison scenarios for the European Alps. *J. Geophys. Res.-Atmos.* **112**, D04105.

Seguí, P. Q., Moigne, P. L., Durand, Y., Martin, E., Habbets, F. and co-authors. 2008. Analysis of near-surface atmospheric variables: validation of SAFRAN analysis over France. *J. Appl. Meteorol. Climatol.* **47**, 769–798.

Semmler, T. and Jacob, D. 2004. Modeling extreme precipitations events—a climate change simulation for Europe. *Global Planet. Change* **44**, 119–127.

Seth, A. and Giorgi, F. 1998. The effect of the domain choice on summer precipitation simulation and sensitivity in a regional climate model. *J. Clim.* **11**, 2698–2712.

Somot, S., Sevault, F., Déqué, M. and Crépon, M. 2008. 21st century climate change scenario for the Mediterranean using a coupled ocean-atmosphere regional climate model. *Global Planet. Change* **63**, 112–126.

von Storch, H., Langenberg, H. and Feser, F. 2000. A spectral nudging technique for dynamical downscaling purposes. *Mon. Wea. Rev.* **128**, 3664–3673.

Waldron, K., Paegle, J. and Horel, J. 1996. Sensitivity of a spectrally filtered and nudged limited area model to outer model options. *Mon. Wea. Rev.* **124**, 529–547.